Statistical emulation of a perturbed basal melt ensemble of an ice sheet model to better quantify Antarctic sea level rise uncertainties

Mira Berdahl[1,3], Gunter Leguy[2], William H. Lipscomb[2], and Nathan M. Urban[3]

[1]Department of Earth and Space Sciences, University of Washington, WA, USA
[2]Climate and Global Dynamics Laboratory, National Center for Atmospheric Research, Boulder, CO, USA
[3]Computational Physics and Methods Group, Los Alamos National Laboratory, Los Alamos, NM 87545, USA

Correspondence: Mira Berdahl (mberdahl@uw.edu)

Abstract. Antarctic ice shelves are vulnerable to warming ocean temperatures, and have already begun thinning in response to increased basal melt rates. Sea level is therefore expected to rise due to Antarctic contributions, but uncertainties in its amount and timing remain largely unquantified. In particular, there is substantial uncertainty in future basal melt rates arising from multi-model differences in thermal forcing and how melt rates depend on that thermal forcing. To facilitate uncertainty quan-

5 tification in sea level rise projections, we build, validate, and demonstrate projections from a computationally efficient statistical emulator of a high resolution (4 km) Antarctic ice sheet model, the Community Ice Sheet Model version 2.1. The emulator is trained to a large (500-member) ensemble of 200-year-long 4-km resolution transient ice sheet simulations, whereby regional basal melt rates are perturbed by idealized (yet physically informed) trajectories. The main advantage of our emulation approach is that by sampling a wide range of possible basal melt trajectories, the emulator can be used to (1) produce prob-

10 abilistic sea level rise projections over much larger Monte Carlo ensembles than are possible by direct numerical simulation alone, thereby providing better statistical characterization of uncertainties, and (2) predict the simulated ice sheet response under differing assumptions about basal melt characteristics as new oceanographic studies are published, without having to run additional numerical ice sheet simulations. As a proof-of-concept, we propagate uncertainties about future basal melt rate trajectories, derived from regional ocean models, to generate probabilistic sea level rise estimates for 100 and 200 years into

15 the future.

1 Introduction

1.1 The physical origin of Antarctic sea level rise uncertainties

Mass loss from Antarctica over the past several decades has primarily been a result of melt at the base of ice shelves (Cook

20 et al., 2016; Rintoul et al., 2016; Pritchard et al., 2012; Rignot and Jacobs, 2002). Depoorter et al. (2013) found that about half of the ice-sheet surface mass gain is lost through oceanic erosion before reaching the ice front. Basal melt weakens the

backforce on upstream glaciers which causes grounding line retreat (Konrad et al., 2018; Rignot et al., 2014), increases flow rate (Pattyn, 2018), depresses surface heights of grounded ice (Konrad et al., 2017), and ultimately impacts sea level. Antarctic ice loss is particularly susceptible to a positive feedback due to the so-called marine ice shelf instability (MISI) (Weertman, 1974; Schoof, 2007). Much of West Antarctica's ice is grounded below sea level, with a retrograde bed sloping downward toward the interior of the continent. MISI theory suggests that increased basal melt rates beneath some key WAIS ice shelves (e.g., Pine Island and Thwaites) could result in an unstable grounding line retreat causing runaway ice loss for the entire region. In fact, there is some evidence through observations and modeling that this process may have already been triggered (Rignot et al., 2014; Joughin et al., 2014; Favier et al., 2014). Forcing due to basal melt is therefore likely to become an increasingly dominant contributor to Antarctic SLR (Bulthuis et al., 2019). Despite its potential to contribute to sea level rise (SLR) vastly more than any other single source (~ 5 m West Antarctica, ~ 60 m all Antarctica), and documented ice shelf thinning (e.g. Schroeder et al., 2019; Reese et al., 2018), Antarctica's contribution to future sea level remains highly uncertain (Heal and Millner, 2014).

The primary unknown in how basal melting will affect sea level rise is the uncertainty in sub-shelf melt rates themselves. Future basal melting is uncertain because it depends on unresolved, coupled ice-ocean processes which are in turn driven by a range of global and regional ocean and atmospheric conditions. Sub-shelf melting can be decomposed into several factors including: changes to the large scale circulation in the Southern Ocean and cross-slope exchange of warm water onto the continental shelf, changes to regional circulation on the shelf, and to the local circulation within ice cavities themselves. Accurately modeling these changes requires high-resolution ocean models in order to link large-scale ocean circulation to sub-shelf melt (Pattyn, 2018; Asay-Davis et al., 2017). Development of these modeling capabilities is still considered the forefront of current research. Most coarse-resolution global models do not have ice shelf cavities, and those that do have large uncertainty regarding changes to the influx of relatively warm Circumpolar Deep Water (CDW) mass into the ice shelf cavities. Ice loss resulting from CDW intrusions has already been observed in the Amundsen Sea region in West Antarctica (Hellmer et al., 2017; Pritchard et al., 2012). Mass loss in the Totten region in East Antarctica has also been linked to ocean circulation changes (Greenbaum et al., 2015; Wouters et al., 2015). There is further uncertainty in how ocean eddies — which are unresolved by current standard-resolution climate models — transport heat to the Antarctic coast (Paolo et al., 2015; Stewart and Thompson, 2015). Finally, outside of basal melt uncertainty, there is deep uncertainty in glaciological dynamics (ie. no consensus on what processes to include in an uncertainty analysis, nor how). An example of this is whether ice fracture mechanics, such as the marine ice cliff instability (MICI), could dramatically accelerate ice loss (DeConto and Pollard, 2016; Edwards et al., 2019).

Efforts by the scientific community have surged in hopes of constraining the uncertainty bounds on future SLR from Antarctica (e.g. initMIP-Antarctica (Seroussi et al., 2019) and ISMIP6 (Seroussi et al., 2020)). The typical approach is to run large ensembles of ice sheet model simulations, perturbing different parameters for each run, and then estimating uncertainty based on the model spread (e.g. Golledge et al., 2015; DeConto and Pollard, 2016). Less conventional techniques have recently been applied, including the use of reduced statistical models (Kopp et al., 2016; Mengel et al., 2016; Fuller et al., 2017; Le Bars et al., 2017) or structured elicitation studies (Kopp et al., 2014; Little et al., 2013; Bamber and Aspinall, 2013). Others have used semi-empirical dynamical models relating GMSL change to global temperature (e.g. Grinsted et al., 2010; Mengel et al.,

2016; Kopp et al., 2016). Others still have used very simple reduced-form mechanistic models such as the BRICK (Building blocks for Relevant Ice and Climate Knowledge) model (Wong et al., 2017) to simulate changes in global mean surface temperature and sea level as a function of perturbations to radiative forcing. Despite this assortment of methods, there is still deep uncertainty in how the ice sheet itself will respond to forcing in the future (Bakker et al., 2017).

1.2 Benefits of statistical emulation of ice sheet models

Kopp et al. (2017) notes that "Ideally, the integration of process models into probabilistic frameworks...would involve the development and use of fast models – or fast statistical emulators of more complex models – in a mode that allows Monte Carlo sampling of key uncertainties and the conditioning of uncertain parameters on multiple observational lines of evidence. The development of such fast models or model emulators is an involved task." Statistical emulators, sometimes referred to as surrogate models, can be used to fully explore parameter space that would otherwise be too computationally intensive for a process-based model. A typical statistical emulation approach is a response-surface formulation — discussed further in Section 2.3 — such as a Gaussian process or neural network, which interpolates the outputs of a perturbed-parameter ensemble of model runs across its input space (Kennedy and O'Hagan, 2001). Because high-fidelity numerical models are computationally expensive, only a limited number of simulations are typically available for the purposes of uncertainty characterization. The goal of an emulator is to inexpensively predict, from a small training ensemble of an expensive computer model, the output that the model would produce if it were run at a new input setting that was too expensive to simulate. The emulator can then be run in much larger ensembles than the original numerical model in order to explore uncertainties.

Statistical emulators have been used in climate science for some time. For example, Hauser et al. (2012) trained and built a Bayesian artificial neural network with GCM output, using their emulators to calibrate climate models against seasonal climatologies of temperature, pressure and humidity. This generated statistically rigorous probabilistic forecasts for future climate states. Not long after, groups began to apply such statistical methods to ice sheet models as a step toward building ice mass loss projections which included uncertainties. For example, Chang et al. (2014) used spatially-resolved synthetic observations (with data-model fusion) to create a probabilistic calibration of a Greenland Ice Sheet model. Recently, emulation has gained even more traction in the Antarctic ice sheet modeling community. Pollard et al. (2016) used a Bayesian technique involving Gaussian process-based emulations and calibration to provide SLR envelopes based on a 3D hybrid ice-sheet model applied to the last deglaciation of WAIS ($\sim 20{,}000$ yr ago). Bulthuis et al. (2019) built an emulator of the continental ice sheet response to a comprehensive set of uncertainties over the next millennium using the Elementary Thermo-mechanical Ice Sheet (f.ETISh) model (Pattyn, 2017) at 20 km resolution. Edwards et al. (2019), built an emulator based on the ice sheet modeling (at 10 km resolution) of DeConto and Pollard (2016) in order to generate probabilistic projections for the Antarctic contribution to sea level rise.

In this paper, we build on these methods by constructing, validating and testing an ice sheet emulator based on the state-of-the-art Community Ice Sheet Model (CISM) version 2.1 (Lipscomb et al., 2019). Our work is novel primarily in its focus on ocean forcing uncertainty in combination with high-resolution glaciological modeling. Specifically:

90 – We focus on uncertainty in ocean forcing, which is considered the most powerful driver of Antarctic sea level rise in the coming centuries.

– We use realistic transient trajectories of basal melt rates that can be mapped back to ocean models, as opposed to more stylized forcings.

– Statistical emulation is applied to the input uncertainty of the (ocean) climate forcing to the ice sheet model, as opposed
95 to the ice model's parameters.

– We use the Community Ice Sheet Model (CISM) at higher resolution (4km) than previously used to construct ice sheet emulators. Benefits of higher resolution ice sheet modeling include, but are not limited to, improved representation of grounding line locations and complex bedrock topography.

– CISM is spun-up in such a way that it is in steady state with the current climate conditions. As such, any forward runs
100 are divorced from issues of drift, so the response can be attributed to forcing and not to internal ice sheet variability.

There are several advantages to our approach of statistically emulating an ice sheet model's response to ocean forcing uncertainty. Conventional approaches to providing basal melt boundary conditions to a standalone ice sheet model include: (1) parameterizing melt rates from the thermal forcing of a global climate model (Naughten et al., 2018; Golledge et al., 2019; Seroussi et al., 2020; Jourdain et al., 2019), (2) using basal melt rates calculated from regional ocean models with ice shelf
105 cavities (Cornford et al., 2015; Timmermann and Hellmer, 2013), or (3) providing stylized forcings such as instantaneous or linear ramp melt trajectories, such as those found in the MISMIP+ and SeaRISE community experiments (Asay-Davis et al., 2016; Bindschadler et al., 2013). Each choice is tied to a specific set of physical/modeling assumptions, and typically does not probe the deep uncertainties in these assumptions.

Our statistical emulation method, by contrast, is intended to be agnostic with respect to these assumptions: we design an ice
110 model ensemble that highly samples a wide range of possible basal melt trajectories (a "space-filling" sampling strategy, to be discussed), initially without consideration of where these trajectories come from or which trajectories are most physically plausible. After constructing a statistical emulator of this ensemble, we can then provide the emulator with basal melt assumptions derived from any scientific source. This has two main advantages: (1) If we change our assumptions about future basal melt rates — due to expert disagreement, new scientific discoveries, or simple sensitivity analysis — we can interrogate the
115 emulator to obtain new Antarctic discharge and sea level rise projections, without having to construct a new set of ice sheet model simulations with new ocean forcings. A corollary is that we can use the emulator as a component in a modeling pipeline that can predict new sea level rise distributions (and their downstream impacts such as coastal flooding) with respect to uncertainties in large-scale climate forcing. (2) We can sample the emulator as many times as we wish, allowing a more complete uncertainty characterization of the distribution of future sea level rise, including extensive sampling into the societally relevant
120 low-probability, high-risk tails of the distribution.

1.3 Outline

The remainder of this paper is structured as follows. In the Methods section, we describe the ice sheet model configuration, ensemble design and the methods to build and validate our Gaussian process emulator. We present results for the CISM ensemble, and then show a simple example of using the emulator to generate a probability distribution function (PDF) of sea

125 level rise by propagating prior distributions of basal melt rate parameters based on fits to two ocean models under the A1B emissions scenario. Figure 1 shows a schematic of the tasks necessary to design, build, validate, and test the Gaussian process emulator.

2 Methods

2.1 Ice sheet model configuration

130 We use CISM, a state-of-the-art 3D, parallel, thermo-mechanical model that runs on a regular mesh grid using a mixture of finite-difference, finite-volume and finite-element methods. As a participant in various ice sheet model intercomparisons (e.g. MISMIP+ (Cornford et al., 2020), LARMIP (Levermann et al., 2019), ABUMIP (Pattyn et al., 2019), and ISMIP6 (Nowicki et al., 2020; Seroussi et al., 2020)), CISM has been shown to perform well compared to other higher-order ice sheet models, some that use resolutions of 1 km or higher in the region containing the grounding line. For the experiments described here,

135 the model was run with the following options:

- A depth-integrated higher-order solver based on Goldberg (2011).

- A basal sliding law based on Schoof (2005), in the power-law limit where the effective pressure is equal to the ice overburden pressure.

- Grounding line parameterizations for basal shear stress and basal melt rate (Leguy et al., 2014).

140 - Application of basal melting to partially floating cells in proportion to the floating fraction of the cell, which is diagnosed from the thickness and basal topography as part of the grounding-line parameterization.

- A no-advance calving criterion that holds the calving front close to its observed location.

- Surface mass balance from late 20th century simulations with the RACMO2 regional climate model (van Wessem et al., 2018).

145 - Geothermal heat flux from Shapiro and Ritzwoller (2004).

The model is spun up over 40,000 years, with the modeled ice thickness nudged toward observed thickness by adjusting a 2D basal friction parameter field beneath grounded ice and basal melt rates beneath floating ice. This inversion scheme is similar to that of Pollard and DeConto (2012)) and was used for the CISM contribution to initMIP-Antarctica (Seroussi et al.,

Task 1: Design
Parameterize future basin-specific basal melt rate trajectories into a family of sigmoidal functions, and widely sample the parameters of the trajectories to generate a space-filling statistical design of ocean forcing scenarios.

Task 2: Run CISM ensemble
Run large Antarctic ice sheet model ensemble over the statistical design, applying basal melt rate anomalies generated from parameterized (500 members, 200 years, 4km resolution).

Task 3: Validation
Validate emulator for key years (100 and 200) using 80% of ensemble data to train emulator and 20% for testing.

Task 4: Generate priors
Use a small set of regional ocean model projections of basal melting as informative probability distributions over the space of ocean forcing trajectories.

Task 5: Emulation
Retrain the emulator on the full 500-member ensemble at key years. Perform Monte Carlo sampling of the emulator predicted future sea level rise over the probability distributions of ocean forcing.

Task 6: Output
The result of Monte Carlo sampling is an emulated probability distribution of cumulative sea level rise after 100 and 200 years of CISM simulation.

Figure 1. Schematic showing step-by-step tasks employed in this emulation study – from experimental design to probabilistic sea level rise output. Figure in Task 2 is adapted from Levermann et al. (2019).
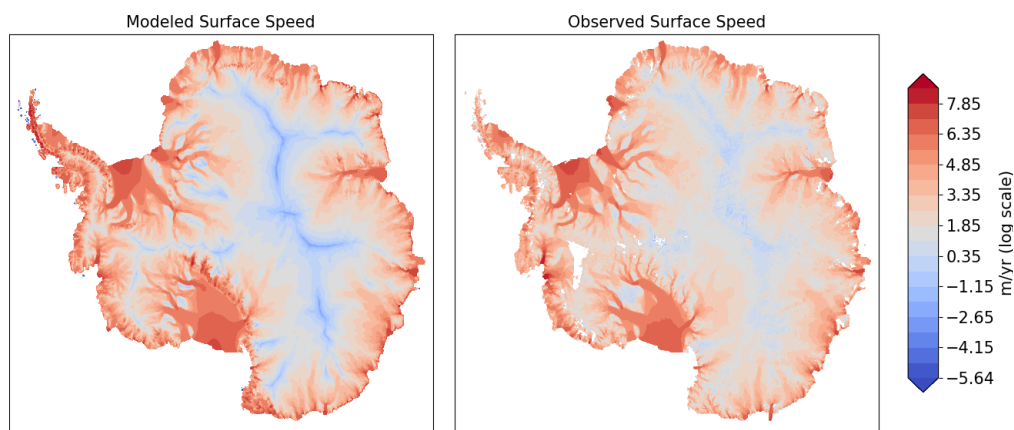
Figure 2. Modeled (left) and observed (right) (Rignot et al., 2011) Antarctic surface speed (m/yr, log scale) at end of spin-up. White patches in the right panel represent missing data.

2019) and the ISMIP6 projections (Nowicki et al., 2020; Seroussi et al., 2020). We note that there is no hydrology in the basal friction field, and the basal melt field is noisy, compensating for other errors in the model or observations. However, this work is a proof-of-concept, and the emulator techniques used here would apply equally well to simulations with more realistic physics. Nudging is strong in the first half of the spin-up, and then tapered off for the second half. The ice thickness gradually approaches a quasi-steady state as basal friction parameters and internal temperatures evolve. The model is run on a uniform 4 km grid, resulting in a spun-up state with excellent agreement between observed and modeled surface velocity (Fig. 2), ice shelf extent, and ice thickness (Fig. 3).

A control run starting from the end of spin-up and going forward 1000 yr (not shown) indicates that there is very little drift in the ice sheet moving forward and that most changes in ice thickness will be a result of forcing as opposed to internal variability or model drift. This is not fully realistic, since the real ice sheet is never truly in equilibrium with the climate, particularly if current observations are used to tune the model. As a result, we consider this model spin-up to be closer to a pre-industrial state, rather than a modern ice sheet. Therefore, henceforth, we do not explicitly state the year corresponding to SLR projections. Rather, we refer to our SLR projections as relative to the number of years run forward in the model from the end of spin-up. As a result, the sea level rise projections are not tied to a particular year in the future. Rather, they are meant to show that the emulator is a powerful and useful tool, and SLR predictions are considered a proof-of-concept.
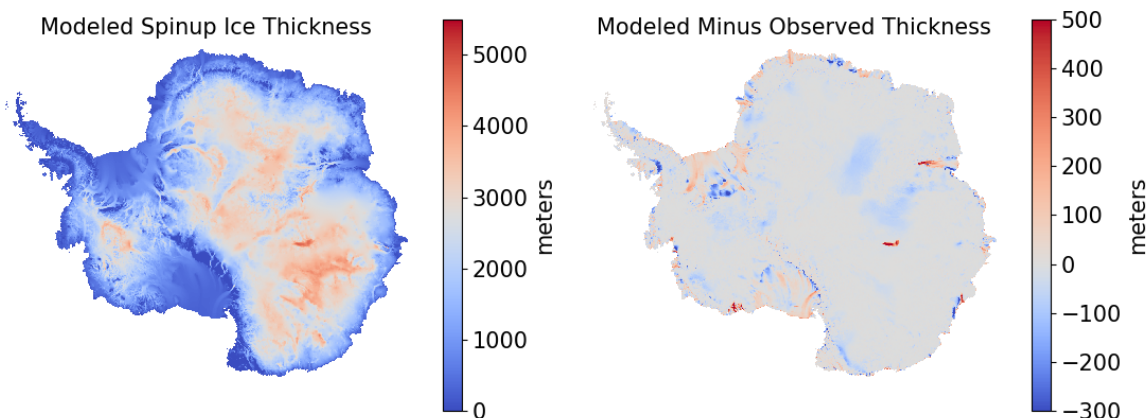
Figure 3. Modeled ice thickness (m) (left) and difference between modeled and observed ice thickness (right). Observations are from the BedMachine Antarctica data set (Morlighem et al., 2020).

2.2 Ensemble Design

165 We use ocean model data from Timmermann and Hellmer (2013) and Cornford et al. (2015) to inform the types of possible basal melt rate trajectory shapes for 200 years forward. The forcing data for the ocean models are generated with the global climate models HadCM3 (Gordon et al., 2000; Collins et al., 2001) and ECHAM5 (Roeckner et al., 2003)) under the A1B and E1 emissions scenarios. (A1B is a moderate scenario similar to Representative Concentration Pathway 6 (RCP6), and E1 is an optimistic, aggressive mitigation scenario.) These are then dynamically downscaled by two high-resolution atmosphere

170 models (RACMO2 and LMDZ4) and two ocean models: the medium resolution BRIOS (Bremerhaven Regional Ice-Ocean Simulation) (Timmermann et al., 2002) and the higher resolution FESOM (Finite-element Sea ice-ocean model) (Wang et al., 2014). We note that the availability of ocean data, particularly melt rate data beyond 2100, was very limited when this study was carried out.

For each CISM ensemble member, we apply a unique basal melt rate anomaly to each of five basins, following the LARMIP
175 region delineation (Levermann et al., 2019). The regions are the Antarctic Peninsula, Weddell Region, East Antarctica, Ross Region, and Amundsen Region (Fig 4). We find that we can accurately capture the behavior of all modeled melt rate shapes

with a sigmoidal function. Figure 5 shows that the sigmoids (colored curves) do an excellent job of characterizing the variety of shapes seen in the ocean model data in each basin. The equation describing the sigmoid is:

$$M(t) = \frac{A}{((1 + e^x)} - B \tag{1}$$

180   where

$$x = -\frac{(t - t_0)}{\tau} \tag{2}$$

$$A = \frac{K}{(K - 1)} \cdot M_{max} \tag{3}$$

$$K = 1 + e^{\left(\frac{t_0}{\tau}\right)} \tag{4}$$

$$B = \frac{A}{K} \tag{5}$$

185   Equation 1 is a function of three independent parameters: t_0 (inflection point of turnover), τ (timescale of turnover), and M_{max} (melt rate to which the function asymptotes). However, because we are only able to constrain the melt rate 200 years into the simulation (we do not have simulations that go out to infinity), we must invert Eq.1 to be in terms of the melt rate at year 200 of the simulation, M_{200}. Using Eqs. 1-5 we can derive coefficients A and B as a function of M_{200}. In doing so, we are able to describe the basal melt trajectories in terms of three parameters: t_0, τ and M_{200}. The emulator is built on these three

190   parameters.

We use a quasi-random Sobol' sequence as a space-filling design method for each parameter (Sobol', 1967). Compared to pseudo-random Monte Carlo sampling, space-filling designs reduce the likelihood of clustering leading to uneven sampling. Sobol' sequences also have an advantage compared to some other common space-filling designs, such as Latin hypercubes (McKay et al., 1979), in that they are sequences designed to fully cover the parameter space at each point, recursively filling

195   the space more densely as points continue to be added to the sequence. This sequential feature of quasi-random sampling allows us to extend the sequence if we desire more ensemble members, while maintaining a space-filling design. A Latin hypercube, by contrast, is not a sequential design and its size must be specified in advance: more points cannot be later added to an existing design without violating the properties of a Latin hypercube.

The ranges for t_0 and τ are determined by maximizing the space-filling properties of the parameters whilst capturing all of

200   the sigmoidal characteristics seen in the modeled ocean melt rate projections in Timmermann and Hellmer (2013) and Cornford et al. (2015). Therefore, using a Sobol' sequence, we sample uniformly between the following lower and upper bounds for the
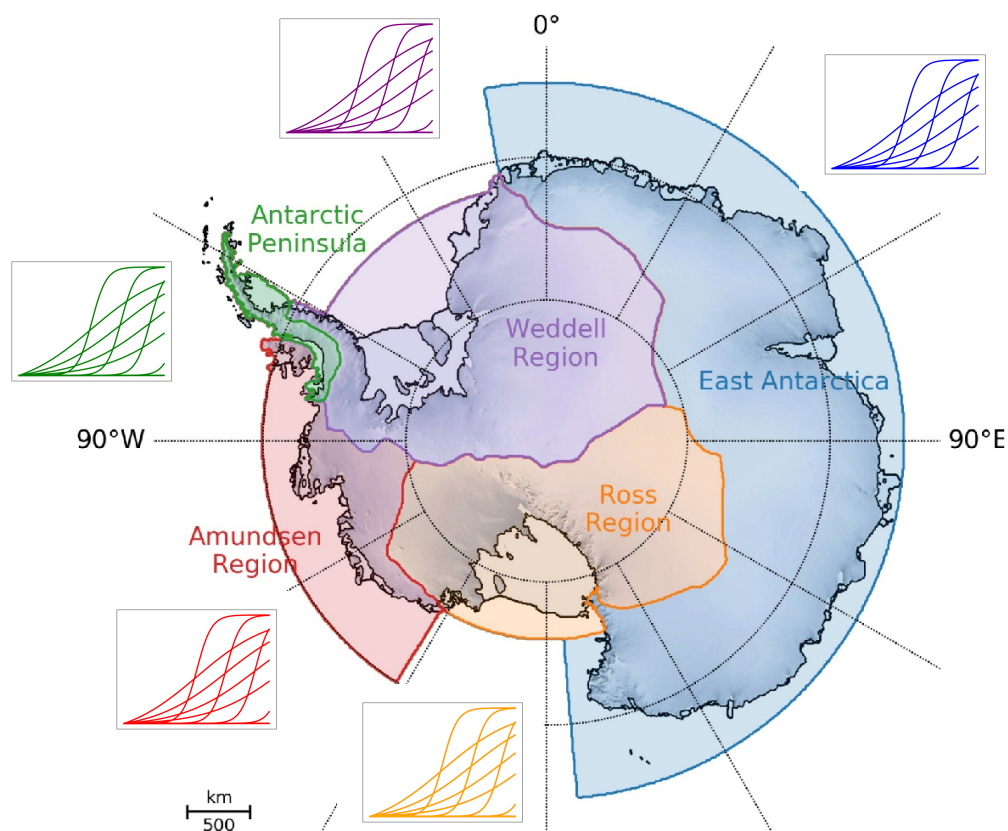
Figure 4. LARMIP regions to which basal melt rate anomalies were applied, adapted from Levermann et al. (2019). Each basin pulls random sigmoid shapes for each ensemble member, with the maximum value at the final year (200) scaled to a basin-specific value, illustrated by the schematized color-coded melt rate trajectories.

sigmoid-defining parameters: $t_0 \in [100{:}225]$, $\tau \in [10{:}75]$, $M_{200} \in [0{:}1]$. M_{200} is later scaled on a basin-by-basin basis (Figure 4, Figure 5), informed by literature values of melt rates at the year 2200 from ocean melt rate projections in Timmermann and Hellmer (2013) and Cornford et al. (2015). Specifically, we allow the M_{200} upper bound to be at least twice the maximum

205 value found in the literature for each basin (shown also in Fig 5). The maximum values imposed for year 200 by basin are therefore:

- Antarctic Peninsula: 12 m/a

- Amundsen Region: 50 m/a

- Ross Region: 20 m/a

210 - East Antarctica: 36 m/a

- Weddell Region: 16 m/a

An example of some basin-specific Sobol' generated sigmoids that would be fed to CISM are shown in Figure 6. For each CISM run, a random basal melt rate curve generated with the Sobol' sequence is chosen for each basin. We have chosen not to assume any correlation between basins. Of course, general ocean warming occurs with global warming, but there may be

215 unique regional circulation patterns that could cause very different basal melt rates in one region compared to another.

We run an ocean-forcing-perturbed CISM ensemble (with 500 members) over the entire Antarctic domain, where CISM surface mass balance is a climatology, and unique ocean melt rate anomalies are added to the background basal melt rates from the end of the CISM spin-up. Since the spun-up basal melt rates are resolved along the ice draft, the original state of basal melt rates has a realistic character, in that it varies along a 2-D surface that is a function of depth so has spatial variability

220 with increasing basal melt rates near the grounding line (Fig 7). We note that by imposing a uniform basal melt rate anomaly for each basin, we are neglecting to account for complex patterns in sub-shelf ocean circulation changes or depth-dependence in the anomaly itself. However, most available melt rate projection data, particularly any estimates that go out 200 years, are regional averages. Furthermore, we must limit the number of parameters we vary in order to be able to run a large enough ensemble to appropriately sample the parameter space and subsequently build an emulator.

225 **2.3 Gaussian Process Emulator of the CISM ice sheet model**

Our knowledge (through observations and modeling) of Antarctic ocean melt rates is changing rapidly, giving rise to frequently revised estimates of sub-shelf melt rates (e.g. through efforts such as ISMIP6 (Nowicki et al., 2020; Seroussi et al., 2020)). Model emulators, or fast surrogates, are useful tools as they allow quick propagation of prior parameter uncertainties through the dynamics of the glaciological system without the need to re-run large ensembles of ice sheet models every time new

230 information about those uncertainties becomes available. Instead, very large Monte Carlo ensembles of surrogate predictions from the emulator, which approximate the ice sheet simulator, can be run in order to highly sample the input uncertainties.
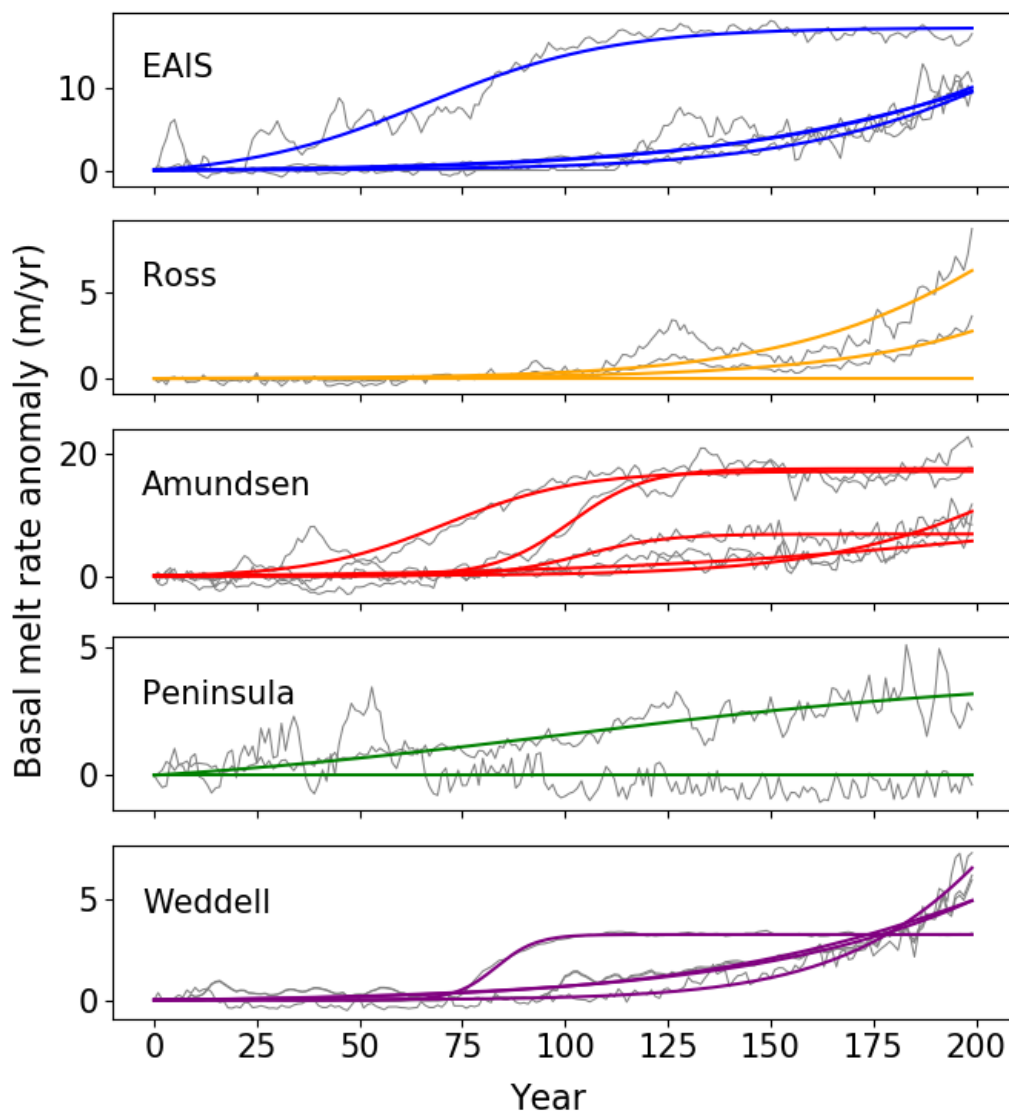
Figure 5. Basal melt rate anomaly data from Timmermann and Hellmer (2013) and Cornford et al. (2015) (grey curves) overlaid with best sigmoidal fits (colored curves). Colors correspond to the LarMIP regions in Figure 4. Note the different y-axis range for each region.
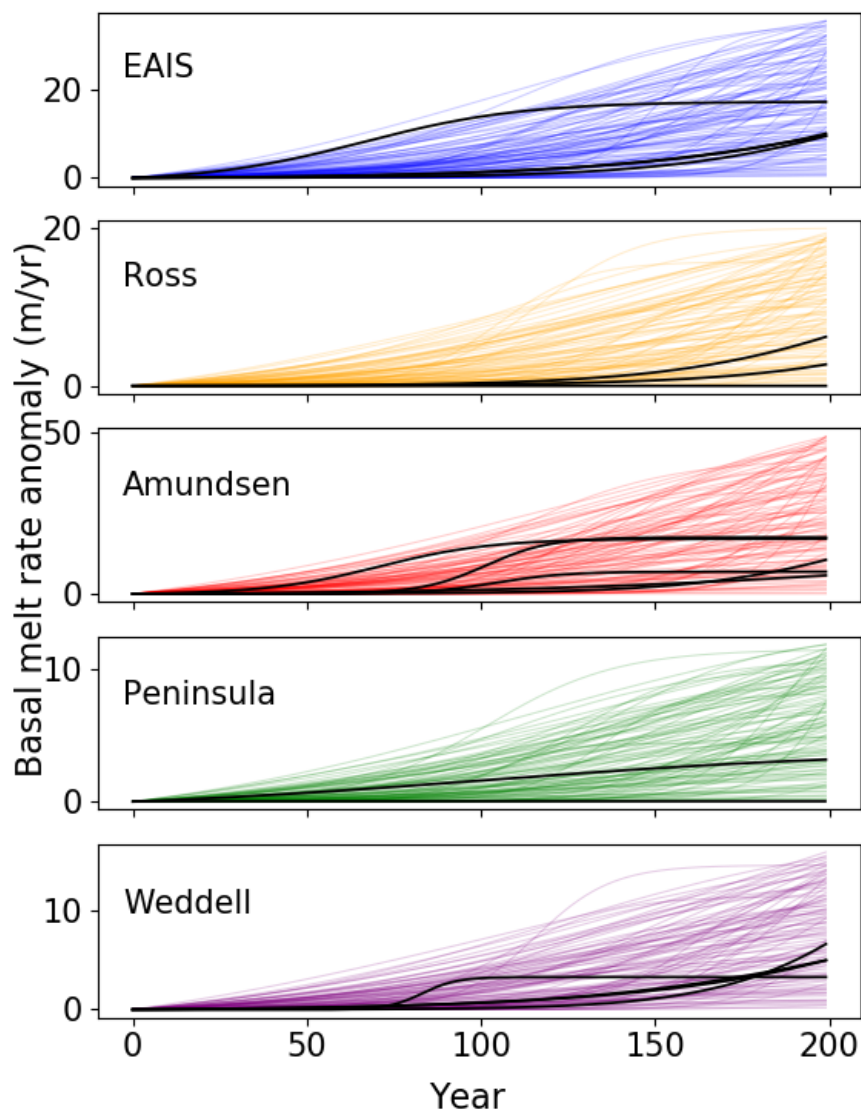
Figure 6. Sample of 100 Sobol'-generated melt rate trajectories (colors) and best fits (by least squares optimization) to ocean model data from Timmermann and Hellmer (2013) and Cornford et al. (2015) overlaid in black for each basin. By definition, the Sobol'-generated curves are permitted to sample up to roughly (sometimes slightly more than) twice the maximum 'data' melt rate at year 200. Note the different y-axis range for each region.
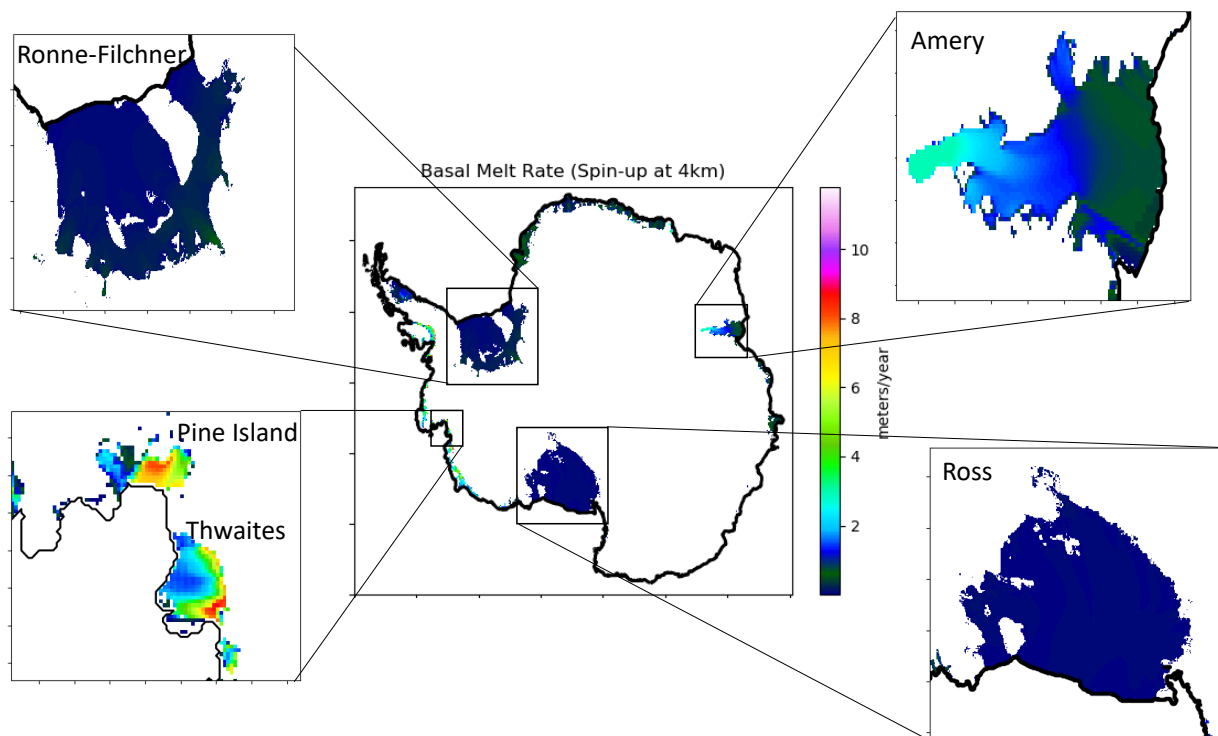
Figure 7. Basal melt rate at end of spin-up at 4km resolution for the all floating ice areas. Zoomed regions include the PIG/Thwaites region, Ronne-Filchner, Amery and Ross ice shelves.

The emulator constructed here predicts a single output (Antarctic SLR anomaly in a specified year of simulation), as a function of a 15-dimensional input vector representing the perturbed regional basal melt trajectories (5 regions x 3 sigmoid parameters, (t_0, τ, M_{200})). The training set is the full 500-member CISM ensemble.

235 Statistical emulation in this paper is of the response surface type (Box and Wilson, 1951). Our training ensemble — consisting of pairs of 15-dimensional input vectors and their corresponding scalar model outputs — can be thought of as samples from a function that maps model inputs to outputs (a response surface). To predict CISM SLR output at a new point in input space, not contained within the training ensemble, a smooth response surface is constructed by interpolating the points in the training set. The emulator prediction for a particular point in input space is the model output interpolated to that point, lying

240 on the response surface.

  The statistical emulator used here is of the popular Gaussian process regression family (Kennedy and O'Hagan, 2001), specifically the implementation found in the 'GPfit' R library (MacDonald et al., 2015). Without going into technical details, Gaussian processes perform nonlinear, multivariate, smooth interpolation of a (potentially irregular) set of training data, which
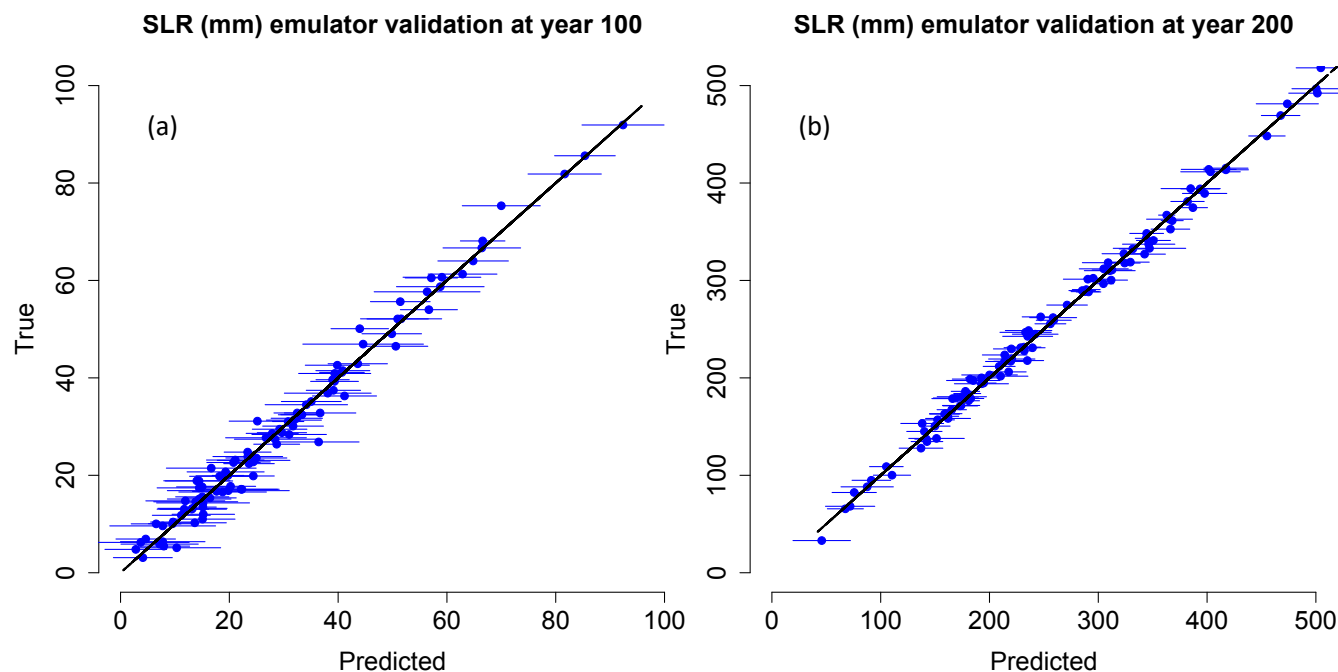
Figure 8. Emulator validation: True (CISM) vs. Predicted (Emulator) SLR values for year 100 (a) and 200 (b). Black solid line shows 1:1 correlation. Correlation coefficients are 0.98 and 0.99 respectively. Note the different x and y scales for (a) and (b).

is computed via a statistical regression procedure. Usually the smoothness of data being fit is estimated as part of the interpo-

245 lating procedure. A Gaussian process's interpolating surface is 'optimal' in a technical sense, going back to the geostatistics literature where it is known as 'kriging' (Matheron, 1962; Krige, 1951). The modern Bayesian interpretation of Gaussian processes provides a second useful statistical feature, namely they can provide the uncertainty in their predictions, i.e., a built-in estimate of interpolation error.

2.3.1 Emulator Validation

250 To validate the emulator, we randomly withhold 20% of the ensemble members, and build an emulator based on the remaining 80% of SLR data from the CISM ensemble. (For the purposes of SLR projection, we train the emulator on the full ensemble.) The emulated SLR values at years 100 and 200 have excellent accuracy with correlation coefficients of 0.98 and 0.99, respectively, against the withheld CISM output (Fig 8). For year 100, 8% of hold-out validation points lie outside the 2-sigma predictive intervals, which is plausible (one would expect 5%). Based on these highly correlated results, we are confident in

255 the emulator's ability to approximate CISM's SLR output 100 and 200 years into the simulation.

3 Results

In this section we present results from the CISM ensemble, showing the SLR contributions at year 100 and 200. We note that the SLR results from the ensemble itself should not be considered physically realistic as the prior melt parameters are uniformly sampled (as described in the Methods Section).

260   We also present results from a simple example illustrating the propagation of parametric uncertainties (M_{200}, t_0 and τ) describing melt rate trajectories (by basin) derived from ocean model projections. These priors are then run through the emulator, resulting in a PDF of SLR at year 100 and 200.

3.1 CISM ensemble results

The CISM ensemble consists of 500 members where each member is forced by five melt rate trajectories, one in each basin.
265 Figure 9 shows the sea level rise time series (top) and corresponding mass loss (Gt/yr) (bottom), resulting from the full 500-member ice sheet ensemble (blue shading), with the ensemble mean shown in red. The distributions of SLR at year 100 are more constrained (ranging from 0.5 – 96 mm) than those in year 200 (ranging from 33 – 543 mm) (Figure 9 top inset). Again, we note that these SLR projections are not physically meaningful since the parameter sampling over which the ensemble is created is uniform. The ensemble is designed purely to be used for the creation of an emulator.

270 3.2 Probabilistic Prediction of Antarctic Sea Level Rise

We test the emulator by running a simple example of prior distributions (based on the FESOM and BRIOS ocean model data described in Timmermann and Hellmer (2013) and Cornford et al. (2015)) through the emulator. We produce a probability density function (PDF) of SLR at years 100 and 200. We generate a distribution of prior parameters based on the 'best fits' found by a least-squares optimization. In the cases that the best fit to a sigmoid has one of the parameters (t_0, τ, or M_{max})
275 near the edge of the allowed parameter range (defined in Section 2.2), we find a fit that is within 1-sigma of the best fit which relaxes the parameter away from the edge of the allowed range. The sigmoid parameters that describe the data fits are then used to generate a normal distribution that serves as the prior.

    The parameter prior distributions in Fig. 10 can be combined and presented as a distribution of sigmoid anomalies (Fig 11). By propagating the priors in Fig 10 for the A1B scenario through the emulator, we can predict SLR probability distributions
280 for year 100 and 200 (Fig 12). The likeliest SLR at year 100 is found to be ~ 7.5 mm. This falls within the range of century-scale future projections of sea level rise from Antarctica in the literature, albeit on the low end of most estimates. The SLR uncertainty in year 100 ranges from 1 mm (2.5%) to 31 mm (97.5%). At year 200, the SLR uncertainty ranges from 37 mm (2.5%) to 255 mm (97.5%).

    As explained in the Model Configuration section, we do not consider this to be a prediction for the year 2100, simply because
285 our spin-up is more in line with a pre-industrial state rather than a modern ice sheet. In the future, one option to eliminate this problem might be to run a historical simulation before the perturbation simulations in order to bring the model into a more sensitive state. However, preliminary attempts to do this with CISM have been focused on global climate model output, which
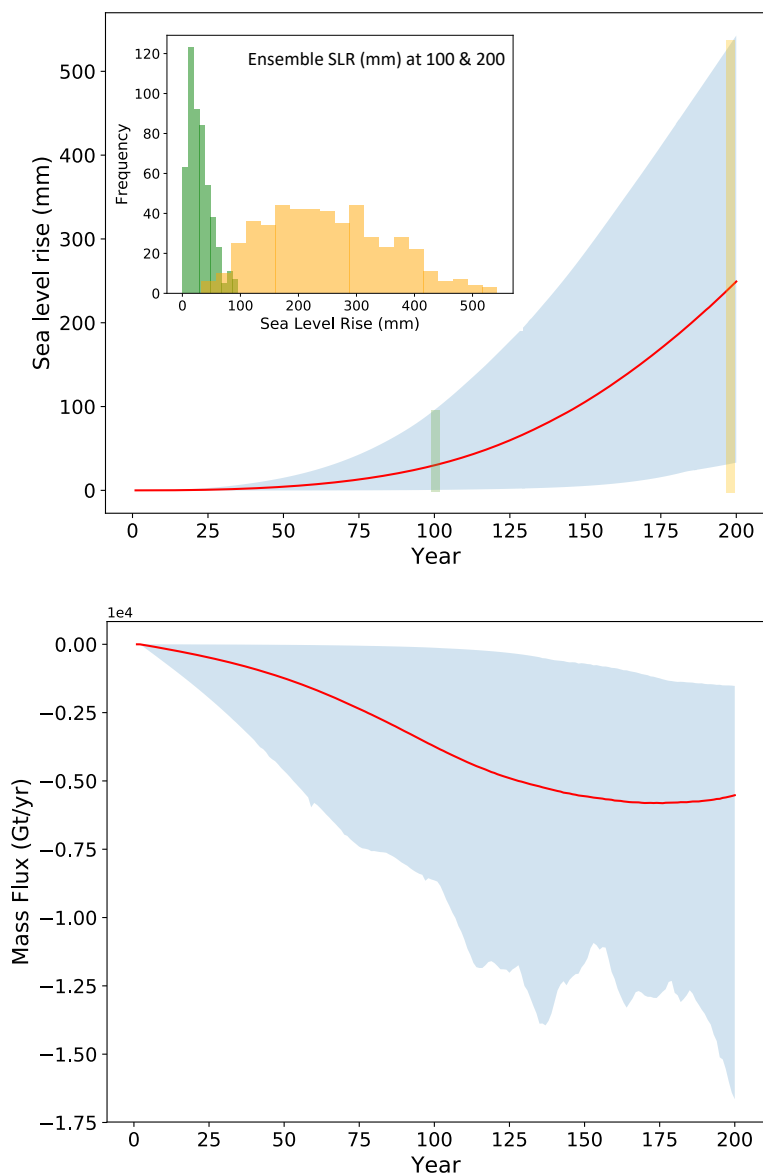
Figure 9. Top: 500-member ensemble SLR contributions (mm) from year 0 to 200, distribution (blue shading) and ensemble mean (red curve). Inset shows sea level rise histogram (mm) at year 100 (green) and 200 (orange) of simulations, corresponding to the vertical green and orange lines in top panel. Note the tighter distributions at year 100 than year 200. Bottom: Mass flux (Gt/yr) of ice during 200 year simulation. Blue shading shows distribution of 500-member ensemble, red curve shows ensemble mean.
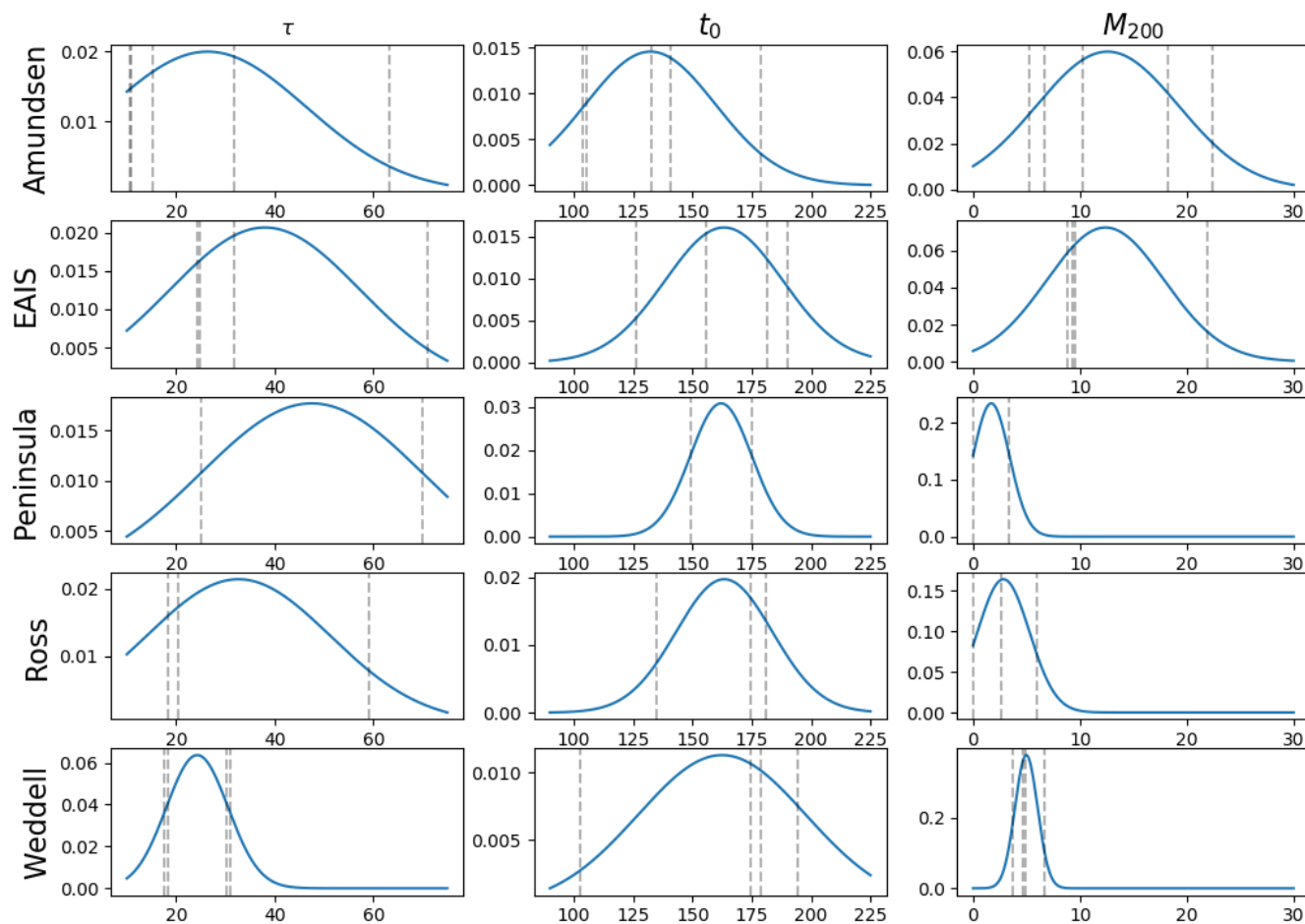
Figure 10. Prior distribution of sigmoid parameters (columns) for each basin (rows). Vertical black dashed lines indicate values that correspond to the 'best fit' to the ocean model data in Timmermann and Hellmer (2013) and Cornford et al. (2015).

did not capture the recent melting in the Amundsun Sea. Another reason for the small response is that the melt rate perturbation is applied uniformly over the basin. Focusing melt near the grounding line (for a given basin mean) would give greater retreat (Lipscomb et al., in review). Section 4 elaborates on both of these points.

4 Discussion and Conclusions

The goal of this work is an in-depth exploration of statistical methods designed to project the effects of a plausible range of sub-shelf ocean forcing conditions upon Antarctic sea level rise uncertainty. We have presented an emulator-based approach to
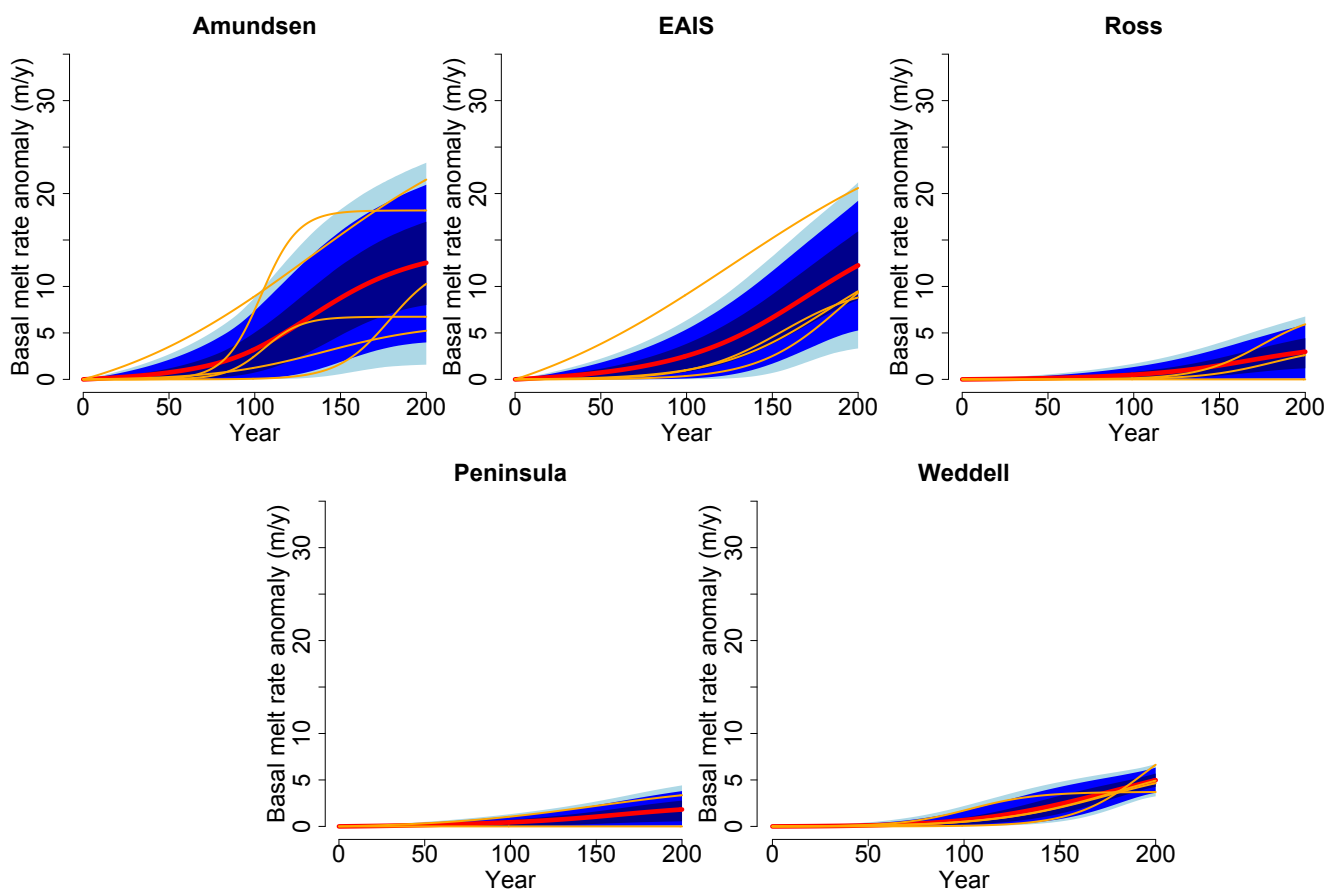
Figure 11. Prior basal melt rate anomaly (m/yr) trajectories as seen by CISM for each region: Amundsen Region, East Antarctic ice sheet (EAIS), Antarctic Peninsula, Ross Region and Weddell Region. Red lines show mean of distribution, blue shaded zones correspond to 50th, 80th and 90th % confidence intervals (from dark blue to light blue respectively), orange lines correspond to best fits (or within 1 sigma of best fit to relax parameters from the edge of their allowable range) to ocean model data.
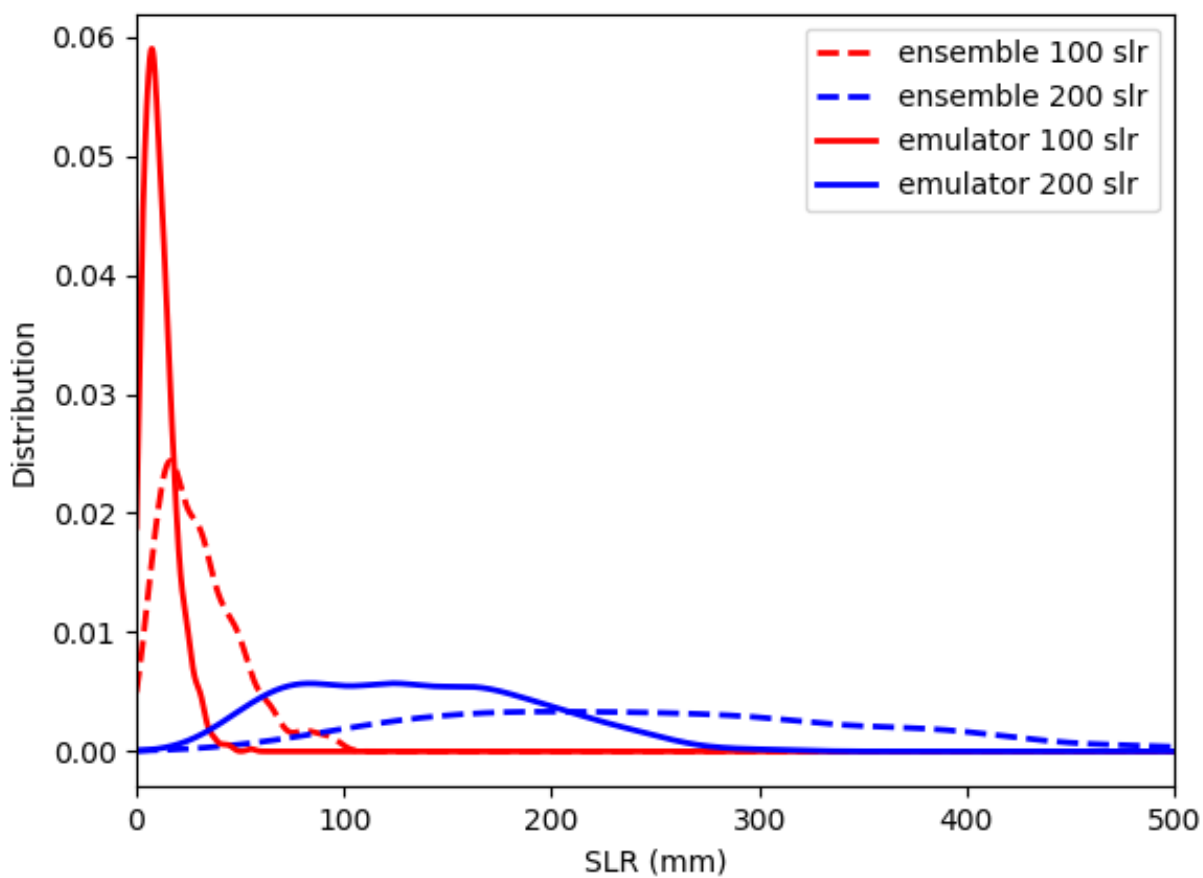
Figure 12. The ensemble SLR PDF at year 100 and 200 (dashed red and blue lines, respectively), and the predicted SLR PDFs for 100 and 200 with the emulator (solid red and blue) for the given prior distributions for the A1B scenario.

derive probabilistic projections of Antarctic sea level rise from a large perturbed basal melt rate ensemble of ice sheet model
simulations.

We designed and ran a 500-member CISM ensemble, perturbing basal melt rates for 200 years over a wide range of possible
future melt trajectories, concentrated on trajectories derived from high-resolution ocean models. With this ice sheet ensemble,
we built and validated a CISM emulator that provides ice retreat as a function of basal melt rate anomalies applied at the
coastal shelves. The main advantage of the emulator is that we can use it to sample a wide range of possible basal melt forcing,
including the high-risk tails of the basal melt projections. The emulator can produce probabilistic sea level rise projections
over much larger Monte Carlo ensembles than are possible by direct numerical simulations alone, thereby providing better
statistical characterization of uncertainties. Furthermore, the emulator can be used to predict the simulated ice sheet response
(along with associated uncertainty bounds) under different assumptions about basal melt rate probability distributions without
running any more dynamic ice sheet simulations. This is especially advantageous as new and updated information becomes
available. Although 200-year CISM simulations are relatively affordable at 4-km resolution, this might not be the case at higher
resolution; each doubling of resolution leads to about a $10\times$ increase in cost. We have further shown how we can propagate
uncertainty through the emulator with a simple example of ocean melt rates under the A1B scenario.

Over a range of future melt-rate trajectories derived from a small collection of high-resolution regional ocean models, the
CISM model projects from 1 mm (2.5%) to 31 mm (97.5%) of Antarctic SLR in year 100 and 37 mm (2.5%) to 255 mm
(97.5%) in year 200. We caution that these results should be interpreted as a proof-of-concept of a method to quantify SLR
uncertainty with respect to uncertainties in ocean forcing, rather than a reliable SLR projection tool. There are several avenues
for improvement.

One important limitation of this study is that we apply a uniform melt rate perturbation to an entire basin, neglecting to
account for melt rate depth-dependence. This assumption could be relaxed in future work, for example, if we were to add (or
swap a sigmoid parameter with) another parameter for ice-ocean physics parameters that control the extent to which melting
is focused near the grounding line. Further improvements would be to increase the ice sheet model resolution, use more
realistic melt parameterizations, and include novel physical mechanics such as hydrofracture and cliff collapse (DeConto and
Pollard, 2016). Eventually, the ice sheet emulator could be included in a larger system linking different sources of uncertainty
with multiple emulators, such as a SLR/coastal flooding integrated assessment. As noted previously, the spin-up we use is
advantageous because it is in equilibrium with the modern forcing and therefore allows us to isolate the effects of forcing as
opposed to model drift in forward runs. However, the drawback of such a spin-up is that one expects the present-day ice sheet
to be out of equilibrium with present-day ocean forcing. Therefore, the model could have a lag in the response to basal melt
rate anomalies, and therefore underestimate future sea level rise.

One way to address this shortfall in future work might be to insert a 'historical forcing' to the spin-up in order to ramp
up the ice sheet to a more sensitive state before applying further basal melt anomalies. Of course, there is still the open
question of how best to parameterize basal melt rates. Incorporating some poorly constrained parameters from current melt rate
parameterizations (e.g. Favier et al., 2019; Jourdain et al., 2019) into the parameter space could be one way to begin unraveling
the uncertainties associated with the parameterizations themselves. Further, the issue remains of how open ocean waters enter

and mix under ice shelves. Despite increased observations and measurements of the Southern Ocean properties in recent years
330 (Newman et al., 2019), sub-shelf circulation and melt processes are still largely unknown in the existing glaciological literature
that focuses on land ice dynamics (Ritz et al., 2015; Pollard et al., 2016).

Another issue we encountered was the lack of data available to use as probability distributions over future basal melt rate
tajectories. This was particularly difficult given our attempt at projecting out 200 years instead of the standard 100 years where
most CMIP5/CMIP6 simulations terminate. One possibility to collect more priors is in the case of moving to a thermal forcing
335 spin-up, such as in Lipscomb et al. (in review). In such a scenario, the ocean forcing consists of thermal forcing anomalies
(derived from ocean temperature and salinity) instead of basal melt rates. The ice sheet model has a parameterization to
convert thermal forcing to melt rates instead of being given melt rates directly. This approach was used for ISMIP6 Antarctic
projections. With such a method, one could use much more data from the CMIP6 dataset, particularly since the ISMIP6 effort
has already generated thermal forcing files for certain projections/models (Jourdain et al., 2019). Again, these data cease at
340 year 2100 but would be a convenient starting point.

Our method for deriving continuous probability distributions over melt rate parameters from a small collection of ocean
models is somewhat ad-hoc. One limitation is that there are many possible, equally good, parameter fits of a sigmoidal curve
to ocean model melt rate trajectory data. Selecting the 'best' fit found by least-squares optimization leads, in some cases,
to parameter estimates on the boundary of the plausible range of values, requiring manual adjustment of the fits. A more
345 principled statistical approach would calculate the full distribution of possible parameter fits to each ocean model, and combine
the distributions found for each ocean model into a single multi-model prior distribution using hierarchical Bayesian model
fusion as in Jonko et al. (2018).

The general issues described above, particularly how to move from coarse (global climate model scale) knowledge of ocean
temperatures to higher resolution sub-shelf melt rates, is a confounding issue in the current state of Antarctic ice sheet modeling.
350 We need global *and* regional ocean models to help address how ocean circulation will change, as well as how eddies transport
water from the open ocean to the continental shelf. Not only do we not know how general increases in ocean temperatures will
translate to sub-shelf melt rates, but also changes in ocean circulation could impact the transport of relatively warm water to
the continental shelf, thereby increasing sub-shelf melt rates as well (e.g. CDW). Progress in this direction will require larger
ensembles of high-resolution regional and global ocean models that sample a wide range of climate scenarios driving Southern
355 Ocean circulation change and variability. Indeed, regional ocean models would be a good target for emulation since these
models are particularly expensive, especially when run beyond a few decades.

Code and data availability. Code and Data are available at: https://github.com/mberdahl-uw/EmulatorPaper

Appendix A

A1

360 *Author contributions.* MB and NU designed the experiments, with input and advice from GL and BL. GL and MB staged the experiments and MB ran them. BL developed and provided an ice sheet spin-up. NU wrote the statistical model that was run by MB. MB prepared the manuscript with contributions from all co-authors.

Competing interests. The authors declare that they have no conflict of interest.

Acknowledgements. Mira Berdahl was supported by the U.S. Department of Energy (DOE) Office of Science (Biological and Environmental
365 Research), Early Career Research program. This material is based upon work supported by the National Center for Atmospheric Research, which is a major facility sponsored by the National Science Foundation under Cooperative Agreement No. 1852977. This research used resources provided by the Los Alamos National Laboratory Institutional Computing Program, which is supported by the U.S. Department of Energy National Nuclear Security Administration under Contract No. 89233218CNA000001. Further computing and data storage resources, including the Cheyenne supercomputer (doi:10.5065/D6RX99HX), were provided by the Computational and Information Systems Labora-
370 tory (CISL) at NCAR. We thank Matthew Hecht for keeping continuity in this work while MB was on maternity leave. MB would like to thank Eric Steig for mentorship and logistical support during this work.

References

Asay-Davis, X. S., Cornford, S. L., Durand, G., Galton-Fenzi, B. K., Gladstone, R. M., Gudmundsson, G. H., Hattermann, T., Holland, D. M., Holland, D., Holland, P. R., et al.: Experimental design for three interrelated marine ice sheet and ocean model intercomparison projects: MISMIP v. 3 (MISMIP+), ISOMIP v. 2 (ISOMIP+) and MISOMIP v. 1 (MISOMIP1), Geoscientific Model Development, 9, 2471–2497, 2016.

Asay-Davis, X. S., Jourdain, N. C., and Nakayama, Y.: Developments in simulating and parameterizing interactions between the Southern Ocean and the Antarctic ice sheet, Current Climate Change Reports, 3, 316–329, 2017.

Bakker, A. M., Louchard, D., and Keller, K.: Sources and implications of deep uncertainties surrounding sea-level projections, Climatic change, 140, 339–347, 2017.

Bamber, J. L. and Aspinall, W.: An expert judgement assessment of future sea level rise from the ice sheets, Nature Climate Change, 3, 424–427, 2013.

Bindschadler, R. A., Nowicki, S., Abe-Ouchi, A., Aschwanden, A., Choi, H., Fastook, J., Granzow, G., Greve, R., Gutowski, G., Herzfeld, U., et al.: Ice-sheet model sensitivities to environmental forcing and their use in projecting future sea level (the SeaRISE project), Journal of Glaciology, 59, 195–224, 2013.

Box, G. and Wilson, K.: On the experimental attainment of optimum conditions, Journal of the Royal Statistical Society, B, 13, 1–45, 1951.

Bulthuis, K., Arnst, M., Sun, S., and Pattyn, F.: Uncertainty quantification of the multi-centennial response of the Antarctic ice sheet to climate change, The Cryosphere, 13, 1349–1380, 2019.

Chang, W., Applegate, P. J., Haran, M., and Keller, K.: Probabilistic calibration of a Greenland Ice Sheet model using spatially resolved synthetic observations: toward projections of ice mass loss with uncertainties, Geoscientific Model Development, 7, 1933–1943, 2014.

Collins, M., Tett, S., and Cooper, C.: The internal climate variability of HadCM3, a version of the Hadley Centre coupled model without flux adjustments, Climate Dynamics, 17, 61–81, 2001.

Cook, A., Holland, P., Meredith, M., Murray, T., Luckman, A., and Vaughan, D.: Ocean forcing of glacier retreat in the western Antarctic Peninsula, Science, 353, 283–286, 2016.

Cornford, S. L., Martin, D. F., Payne, A. J., Ng, E. G., Le Brocq, A. M., Gladstone, R. M., Edwards, T. L., Shannon, S. R., Agosta, C., van den Broeke, M. R., Hellmer, H. H., Krinner, G., Ligtenberg, S. R. M., Timmermann, R., and Vaughan, D. G.: Century-scale simulations of the response of the West Antarctic Ice Sheet to a warming climate, The Cryosphere, 9, 1579–1600, https://doi.org/10.5194/tc-9-1579-2015, https://www.the-cryosphere.net/9/1579/2015/, 2015.

Cornford, S. L., Seroussi, H., Asay-Davis, X. S., Gudmundsson, G. H., Arthern, R., Borstad, C., Christmann, J., Dias dos Santos, T., Feldmann, J., Goldberg, D., et al.: Results of the third Marine Ice Sheet Model Intercomparison Project (MISMIP+), The Cryosphere Discussions, 2020.

DeConto, R. M. and Pollard, D.: Contribution of Antarctica to past and future sea-level rise, Nature, 531, 591, 2016.

Depoorter, M. A., Bamber, J., Griggs, J., Lenaerts, J., Ligtenberg, S. R., Van den Broeke, M., and Moholdt, G.: Calving fluxes and basal melt rates of Antarctic ice shelves, Nature, 502, 89, 2013.

Edwards, T. L., Brandon, M. A., Durand, G., Edwards, N. R., Golledge, N. R., Holden, P. B., Nias, I. J., Payne, A. J., Ritz, C., and Wernecke, A.: Revisiting Antarctic ice loss due to marine ice-cliff instability, Nature, 566, 58–64, 2019.

Favier, L., Durand, G., Cornford, S. L., Gudmundsson, G. H., Gagliardini, O., Gillet-Chaulet, F., Zwinger, T., Payne, A., and Le Brocq, A. M.: Retreat of Pine Island Glacier controlled by marine ice-sheet instability, Nature Climate Change, 4, 117–121, 2014.

Favier, L., Jourdain, N. C., Jenkins, A., Merino, N., Durand, G., Gagliardini, O., Gillet-Chaulet, F., and Mathiot, P.: Assessment of sub-shelf
melting parameterisations using the ocean–ice-sheet coupled model NEMO (v3. 6)–Elmer/Ice (v8. 3), Geoscientific Model Development,
12, 2255–2283, 2019.

Fuller, R. W., Wong, T. E., and Keller, K.: Probabilistic inversion of expert assessments to inform projections about Antarctic ice sheet
responses, PloS one, 12, 2017.

Goldberg, D. N.: A variationally derived, depth-integrated approximation to a higher-order glaciological flow model, Journal of Glaciology,
57, 157–170, 2011.

Golledge, N. R., Kowalewski, D. E., Naish, T. R., Levy, R. H., Fogwill, C. J., and Gasson, E. G.: The multi-millennial Antarctic commitment
to future sea-level rise, Nature, 526, 421–425, 2015.

Golledge, N. R., Keller, E. D., Gomez, N., Naughten, K. A., Bernales, J., Trusel, L. D., and Edwards, T. L.: Global environmental conse-
quences of twenty-first-century ice-sheet melt, Nature, 566, 65–72, 2019.

Gordon, C., Cooper, C., Senior, C. A., Banks, H., Gregory, J. M., Johns, T. C., Mitchell, J. F., and Wood, R. A.: The simulation of SST, sea
ice extents and ocean heat transports in a version of the Hadley Centre coupled model without flux adjustments, Climate dynamics, 16,
147–168, 2000.

Greenbaum, J., Blankenship, D., Young, D., Richter, T., Roberts, J., Aitken, A., Legresy, B., Schroeder, D., Warner, R., Van Ommen, T.,
et al.: Ocean access to a cavity beneath Totten Glacier in East Antarctica, Nature Geoscience, 8, 294–298, 2015.

Grinsted, A., Moore, J. C., and Jevrejeva, S.: Reconstructing sea level from paleo and projected temperatures 200 to 2100 AD, Climate
dynamics, 34, 461–472, 2010.

Hauser, T., Keats, A., and Tarasov, L.: Artificial neural network assisted Bayesian calibration of climate models, Climate dynamics, 39,
137–154, 2012.

Heal, G. and Millner, A.: Reflections: Uncertainty and decision making in climate change economics, Review of Environmental Economics
and Policy, 8, 120–137, 2014.

Hellmer, H. H., Kauker, F., Timmermann, R., and Hattermann, T.: The fate of the southern Weddell Sea continental shelf in a warming
climate, Journal of Climate, 30, 4337–4350, 2017.

Jonko, A., Urban, N. M., and Nadiga, B.: Towards Bayesian hierarchical inference of equilibrium climate sensitivity from a combination of
CMIP5 climate models and observational data, Climatic Change, 149, 247–260, 2018.

Joughin, I., Smith, B. E., and Medley, B.: Marine ice sheet collapse potentially under way for the Thwaites Glacier Basin, West Antarctica,
Science, 344, 735–738, 2014.

Jourdain, N. C., Asay-Davis, X., Hattermann, T., Straneo, F., Seroussi, H., Little, C. M., and Nowicki, S.: A protocol for calculating basal
melt rates in the ISMIP6 Antarctic ice sheet projections, The Cryosphere Discuss., https://doi. org/10.5194/tc-2019-277, in review, 2019.

Kennedy, M. C. and O'Hagan, A.: Bayesian calibration of computer models, Journal of the Royal Statistical Society: Series B (Statistical
Methodology), 63, 425–464, 2001.

Konrad, H., Gilbert, L., Cornford, S. L., Payne, A., Hogg, A., Muir, A., and Shepherd, A.: Uneven onset and pace of ice-dynamical imbalance
in the Amundsen Sea Embayment, West Antarctica, Geophysical Research Letters, 44, 910–918, 2017.

Konrad, H., Shepherd, A., Gilbert, L., Hogg, A. E., McMillan, M., Muir, A., and Slater, T.: Net retreat of Antarctic glacier grounding lines,
Nature Geoscience, 11, 258, 2018.

Kopp, R. E., Horton, R. M., Little, C. M., Mitrovica, J. X., Oppenheimer, M., Rasmussen, D., Strauss, B. H., and Tebaldi, C.: Probabilistic
21st and 22nd century sea-level projections at a global network of tide-gauge sites, Earth's future, 2, 383–406, 2014.

Kopp, R. E., Kemp, A. C., Bittermann, K., Horton, B. P., Donnelly, J. P., Gehrels, W. R., Hay, C. C., Mitrovica, J. X., Morrow, E. D., and Rahmstorf, S.: Temperature-driven global sea-level variability in the Common Era, Proceedings of the National Academy of Sciences, 113, E1434–E1441, 2016.

Kopp, R. E., DeConto, R. M., Bader, D. A., Hay, C. C., Horton, R. M., Kulp, S., Oppenheimer, M., Pollard, D., and Strauss, B. H.: Evolving understanding of Antarctic ice-sheet physics and ambiguity in probabilistic sea-level projections, Earth's Future, 5, 1217–1233, 2017.

Krige, D. G.: A statistical approach to some mine valuation and allied problems on the Witwatersrand: By DG Krige, Ph.D. thesis, University of the Witwatersrand, 1951.

Le Bars, D., Drijfhout, S., and de Vries, H.: A high-end sea level rise probabilistic projection including rapid Antarctic ice sheet mass loss, Environmental Research Letters, 12, 044 013, 2017.

Leguy, G. R., Asay-Davis, X. S., and Lipscomb, W. H.: Parameterization of basal friction near grounding lines in a one-dimensional ice sheet model, The Cryosphere, 8, 1239–1259, https://doi.org/10.5194/tc-8-1239-2014, 2014.

Levermann, A., Winkelmann, R., Albrecht, T., Goelzer, H., Golledge, N. R., Greve, R., Huybrechts, P., Jordan, J., Leguy, G., Martin, D., Morlighem, M., Pattyn, F., Pollard, D., Quiquet, A., Rodehacke, C., Seroussi, H., Sutter, J., Zhang, T., Van Breedam, J., DeConto, R., Dumas, C., Garbe, J., Gudmundsson, G. H., Hoffman, M. J., Humbert, A., Kleiner, T., Lipscomb, W., Meinshausen, M., Ng, E., Perego, M., Price, S. F., Saito, F., Schlegel, N.-J., Sun, S., and van de Wal, R. S. W.: Projecting Antarctica's contribution to future sea level rise from basal ice-shelf melt using linear response functions of 16 ice sheet models (LARMIP-2), Earth System Dynamics Discussions, 2019, 1–63, https://doi.org/10.5194/esd-2019-23, https://www.earth-syst-dynam-discuss.net/esd-2019-23/, 2019.

Lipscomb, W. H., Price, S. F., Hoffman, M. J., Leguy, G. R., Bennett, A. R., Bradley, S. L., Evans, K. J., Fyke, J. G., Kennedy, J. H., Perego, M., et al.: Description and evaluation of the Community Ice Sheet Model (CISM) v2. 1, Geoscientific Model Development, 12, 387–424, 2019.

Lipscomb, W. H., Leguy, G. R., Jourdain, N. C., Asay-Davis, X., Seroussi, H., and Nowicki, S.: ISMIP6 projections of ocean-forced Antarctic Ice Sheet evolution using the Community Ice Sheet Model, in review at The Cryosphere, in review.

Little, C. M., Oppenheimer, M., and Urban, N. M.: Upper bounds on twenty-first-century Antarctic ice loss assessed using a probabilistic framework, Nature Climate Change, 3, 654–659, 2013.

MacDonald, B., Ranjan, P., and Chipman, H.: GPfit: An R Package for Fitting a Gaussian Process Model to Deterministic Simulator Outputs, Journal of Statistical Software, 64, 1–23, http://www.jstatsoft.org/v64/i12/, 2015.

Matheron, G.: Traité de géostatistique appliquée. 1 (1962), vol. 1, Editions Technip, 1962.

McKay, M. D., Beckman, R. J., and Conover, W. J.: Comparison of three methods for selecting values of input variables in the analysis of output from a computer code, Technometrics, 21, 239–245, 1979.

Mengel, M., Levermann, A., Frieler, K., Robinson, A., Marzeion, B., and Winkelmann, R.: Future sea level rise constrained by observations and long-term commitment, Proceedings of the National Academy of Sciences, 113, 2597–2602, 2016.

Morlighem, M., Rignot, E., Binder, T., Blankenship, D., Drews, R., Eagles, G., Eisen, O., Ferraccioli, F., Forsberg, R., Fretwell, P., et al.: Deep glacial troughs and stabilizing ridges unveiled beneath the margins of the Antarctic ice sheet, Nature Geoscience, 13, 132–137, 2020.

Naughten, K. A., Meissner, K. J., Galton-Fenzi, B. K., England, M. H., Timmermann, R., and Hellmer, H. H.: Future projections of Antarctic ice shelf melting based on CMIP5 scenarios, Journal of Climate, 31, 5243–5261, 2018.

Newman, L., Heil, P., Trebilco, R., Katsumata, K., Constable, A., van Wijk, E., Assmann, K., Beja, J., Bricher, P., Coleman, R., et al.: Delivering sustained, coordinated, and integrated observations of the southern ocean for global impact, Frontiers in Marine Science, 6, 433, 2019.

485 Nowicki, S., Payne, A. J., Goelzer, H., Seroussi, H., Lipscomb, W. H., Abe-Ouchi, A., Agosta, C., Alexander, P., Asay-Davis, X. S., Barthel, A., Bracegirdle, T. J., Cullather, R., Felikson, D., Fettweis, X., Gregory, J., Hatterman, T., Jourdain, N. C., Kuipers Munneke, P., Larour, E., Little, C. M., Morlinghem, M., Nias, I., Shepherd, A., Simon, E., Slater, D., Smith, R., Straneo, F., Trusel, L. D., van den Broeke, M. R., and van de Wal, R.: Experimental protocol for sealevel projections from ISMIP6 standalone ice sheet models, The Cryosphere Discussions, 2020, 1–40, https://doi.org/10.5194/tc-2019-322, https://www.the-cryosphere-discuss.net/tc-2019-322/, 2020.

490 Paolo, F. S., Fricker, H. A., and Padman, L.: Volume loss from Antarctic ice shelves is accelerating, Science, 348, 327–331, 2015.

Pattyn, F.: Sea-level response to melting of Antarctic ice shelves on multi-centennial timescales with the fast Elementary Thermomechanical Ice Sheet model (f. ETISh v1. 0)., Cryosphere, 11, 2017.

Pattyn, F.: The paradigm shift in Antarctic ice sheet modelling, Nature communications, 9, 2728, 2018.

Pattyn, F., Sun, S., and Simon, E.: Influence of ice-shelf collapse on Antarctic grounding-line dynamics: results from ABUMIP., in: Geo-
495 physical Research Abstracts, vol. 21, 2019.

Pollard, D. and DeConto, R.: A simple inverse method for the distribution of basal sliding coefficients under ice sheets, applied to Antarctica, The Cryosphere, 6, 953, 2012.

Pollard, D., Chang, W., Haran, M., Applegate, P., and DeConto, R.: Large ensemble modeling of the last deglacial retreat of the West Antarctic Ice Sheet: comparison of simple and advanced statistical techniques, 2016.

500 Pritchard, H., Ligtenberg, S. R., Fricker, H. A., Vaughan, D. G., van den Broeke, M. R., and Padman, L.: Antarctic ice-sheet loss driven by basal melting of ice shelves, Nature, 484, 502–505, 2012.

Reese, R., Gudmundsson, G. H., Levermann, A., and Winkelmann, R.: The far reach of ice-shelf thinning in Antarctica, Nature Climate Change, 8, 53–57, 2018.

Rignot, E. and Jacobs, S. S.: Rapid bottom melting widespread near Antarctic ice sheet grounding lines, Science, 296, 2020–2023, 2002.

505 Rignot, E., Mouginot, J., and Scheuchl, B.: Ice flow of the Antarctic ice sheet, Science, 333, 1427–1430, 2011.

Rignot, E., Mouginot, J., Morlighem, M., Seroussi, H., and Scheuchl, B.: Widespread, rapid grounding line retreat of Pine Island, Thwaites, Smith, and Kohler glaciers, West Antarctica, from 1992 to 2011, Geophysical Research Letters, 41, 3502–3509, 2014.

Rintoul, S. R., Silvano, A., Pena-Molino, B., van Wijk, E., Rosenberg, M., Greenbaum, J. S., and Blankenship, D. D.: Ocean heat drives rapid basal melt of the Totten Ice Shelf, Science Advances, 2, e1601 610, 2016.

510 Ritz, C., Edwards, T. L., Durand, G., Payne, A. J., Peyaud, V., and Hindmarsh, R. C.: Potential sea-level rise from Antarctic ice-sheet instability constrained by observations, Nature, 528, 115, 2015.

Roeckner, E., Bäuml, G., Bonaventura, L., Brokopf, R., Esch, M., Giorgetta, M., Hagemann, S., Kirchner, I., Kornblueh, L., Manzini, E., et al.: The atmospheric general circulation model ECHAM 5. PART I: Model description, 2003.

Schoof, C.: The effect of cavitation on glacier sliding, Proceedings of the Royal Society A: Mathematical, Physical and Engineering Sciences,
515 461, 609–627, 2005.

Schoof, C.: Marine ice-sheet dynamics. Part 1. The case of rapid sliding, Journal of Fluid Mechanics, 573, 27–55, 2007.

Schroeder, D. M., Dowdeswell, J. A., Siegert, M. J., Bingham, R. G., Chu, W., MacKie, E. J., Siegfried, M. R., Vega, K. I., Emmons, J. R., and Winstein, K.: Multidecadal observations of the Antarctic ice sheet from restored analog radar records, Proceedings of the National Academy of Sciences, 116, 18 867–18 873, 2019.

520 Seroussi, H., Nowicki, S., Simon, E., Abe-Ouchi, A., Albrecht, T., Brondex, J., Cornford, S., Dumas, C., Gillet-Chaulet, F., Goelzer, H., et al.: initMIP-Antarctica: an ice sheet model initialization experiment of ISMIP6, The Cryosphere, 13, 1441–1471, 2019.

Seroussi, H., Nowicki, S., Payne, A. J., Goelzer, H., Lipscomb, W. H., Abe Ouchi, A., Agosta, C., Albrecht, T., Asay-Davis, X., Barthel, A., Calov, R., Cullather, R., Dumas, C., Gladstone, R., Golledge, N., Gregory, J. M., Greve, R., Hatterman, T., Hoffman, M. J., Humbert, A., Huybrechts, P., Jourdain, N. C., Kleiner, T., Larour, E., Leguy, G. R., Lowry, D. P., Little, C. M., Morlighem, M., Pattyn, F., Pelle, T., Price,
525   S. F., Quiquet, A., Reese, R., Schlegel, N.-J., Shepherd, A., Simon, E., Smith, R. S., Straneo, F., Sun, S., Trusel, L. D., Van Breedam, J., van de Wal, R. S. W., Winkelmann, R., Zhao, C., Zhang, T., and Zwinger, T.: ISMIP6 Antarctica: a multi-model ensemble of the Antarctic ice sheet evolution over the 21st century, The Cryosphere Discussions, 2020, 1–54, https://doi.org/10.5194/tc-2019-324, https://www.the-cryosphere-discuss.net/tc-2019-324/, 2020.

Shapiro, N. and Ritzwoller, M.: Inferring surface heat flux distributions guided by a global seismic model: particular application to Antarctica,
530   Earth Planet. Sci. Lett., 223, 213–224, https://doi.org/10.1016/j.epsl.2004.04.011, 2004.

Sobol', I. M.: On the distribution of points in a cube and the approximate evaluation of integrals, Zhurnal Vychislitel'noi Matematiki i Matematicheskoi Fiziki, 7, 784–802, 1967.

Stewart, A. L. and Thompson, A. F.: Eddy-mediated transport of warm Circumpolar Deep Water across the Antarctic shelf break, Geophysical Research Letters, 42, 432–440, 2015.

535   Timmermann, R. and Hellmer, H. H.: Southern Ocean warming and increased ice shelf basal melting in the twenty-first and twenty-second centuries based on coupled ice-ocean finite-element modelling, Ocean Dynamics, 63, 1011–1026, https://doi.org/10.1007/s10236-013-0642-0, https://doi.org/10.1007/s10236-013-0642-0, 2013.

Timmermann, R., Beckmann, A., and Hellmer, H.: Simulations of ice-ocean dynamics in the Weddell Sea 1. Model configuration and validation, Journal of Geophysical Research: Oceans, 107, 10–1, 2002.

540   van Wessem, J. M., Jan Van De Berg, W., Noël, B. P., Van Meijgaard, E., Amory, C., Birnbaum, G., Jakobs, C. L., Krüger, K., Lenaerts, J., Lhermitte, S., et al.: Modelling the climate and surface mass balance of polar ice sheets using RACMO2: Part 2: Antarctica (1979-2016), Cryosphere, 12, 1479–1498, 2018.

Wang, Q., Danilov, S., Sidorenko, D., Timmermann, R., Wekerle, C., Wang, X., Jung, T., and Schröter, J.: The Finite Element Sea Ice-Ocean Model (FESOM) v. 1.4: formulation of an ocean general circulation model, Geoscientific Model Development, 7, 663–693, 2014.

545   Weertman, J.: Stability of the junction of an ice sheet and an ice shelf, Journal of Glaciology, 13, 3–11, 1974.

Wong, T. E., Bakker, A. M., Ruckert, K., Applegate, P., Slangen, A. B., and Keller, K.: BRICK v0. 2, a simple, accessible, and transparent model framework for climate and regional sea-level projections, Geoscientific Model Development, 10, 2741, 2017.

Wouters, B., Martin-Español, A., Helm, V., Flament, T., van Wessem, J. M., Ligtenberg, S. R., Van den Broeke, M. R., and Bamber, J. L.: Dynamic thinning of glaciers on the Southern Antarctic Peninsula, Science, 348, 899–903, 2015.